OMTO, Volume *25*

Supplemental information

Amplification of the CXCR3/CXCL9 axis via intratumoral electroporation of plasmid CXCL9 synergizes with plasmid IL-12 therapy to elicit robust anti-tumor immunity

Jack Y. Lee, Bianca Nguyen, Anandaroop Mukhopadhyay, Mia Han, Jun Zhang, Ravindra Gujar, Jon Salazar, Reneta Hermiz, Lauren Svenson, Erica Browning, H. Kim Lyerly, David A. Canton, Daniel Fisher, Adil Daud, Alain Algazi, Joseph Skitzki, and Christopher G. Twitty

Supplemental Materials and Methods:

RNA extraction and gene expression analysis

GPCRs:

Gpsm3, Jak3, Adgre1, Ccl5, Il2ra, Cxcl16, Il2rg, Ccl9, Il2rb, Ccr2, Ccr5, Cxcl9, Pik3r1, Jak2, Jak1, Cxcr6, Cxcl10, Cxcl2, Rock1, Akt1, Pf4, Prkacb, Cxcr4, Cmklr1, Pik3ca, Csf2rb, Pik3r2, Ccl4, Cxcl5, Cxcl12, Cxcl3, Nras, Pik3cg, Apoe, C5ar1, Adm, Ccl6, Kras

Interleukins:

Jak3, Nfkbia, Il18bp, Il12b, Csf1r, Il2ra, Casp1, Il2rg, Chuk, Il2rb, Psmb9, Stat1, Psmb8, Map3k7, Stat6, Pik3r1, Jak2, Nfkb1, Jak1, Ikbkg, Csf1, Hmgb1, Socs1, Stat2, Il7r, Lck, Ptpn11-, Il1b, Il21r, Il1rn, Il10ra, Pik3ca, Csf2rb, Pik3r2, Map3k8, Il6ra, Syk, Ikbkb, Psmb5, Il33, Hck, Myd88, Il18, Ripk2, Fyn, Il1r2, Rela, Casp3

Interferons:

Ifngr2, Ifngr1, Isg15, Stat1, Ifnar1, Uba7, Jak2, Jak1, Irf3, Socs1, Eif2ak2, Stat2, Irf9, Ptpn11

MHC I:

Cybb, Fcgr1, H2-D1, Dtx3l, Herc6, Cd36, Psmb9, Fcgr1, Uba7, Psmb8, Mrc1, B2m, H2-T23, Tap2, Elob, Cdc20, Socs1, H2-M3, Psmb5, Trim21

CD28:

H2-Ab1, H2-Aa, H2-Eb1, Tnfrsf14, Rictor, Cd274, Pik3r1, Cd3d, Cd247, Pdcd1, Cd28, Cd3g, Akt1, Lck, Ptpn11, Icos, Pik3ca, Cd86, Pik3r2, Map3k8, Fyn, Mtor

TCR:

H2-Ab1, Nfkbia, H2-Aa, H2-Eb1, Chuk, Psmb9, Psmb8, Map3k7, Pik3r1, Cd3d, Nfkb1, Ikbkg, Cd247, Zap70, Cd3g, Lck, Pik3ca, Pik3r2, Ikbkb, Psmb5, Pten, Ripk2, Rela

Supplementary Figure 1

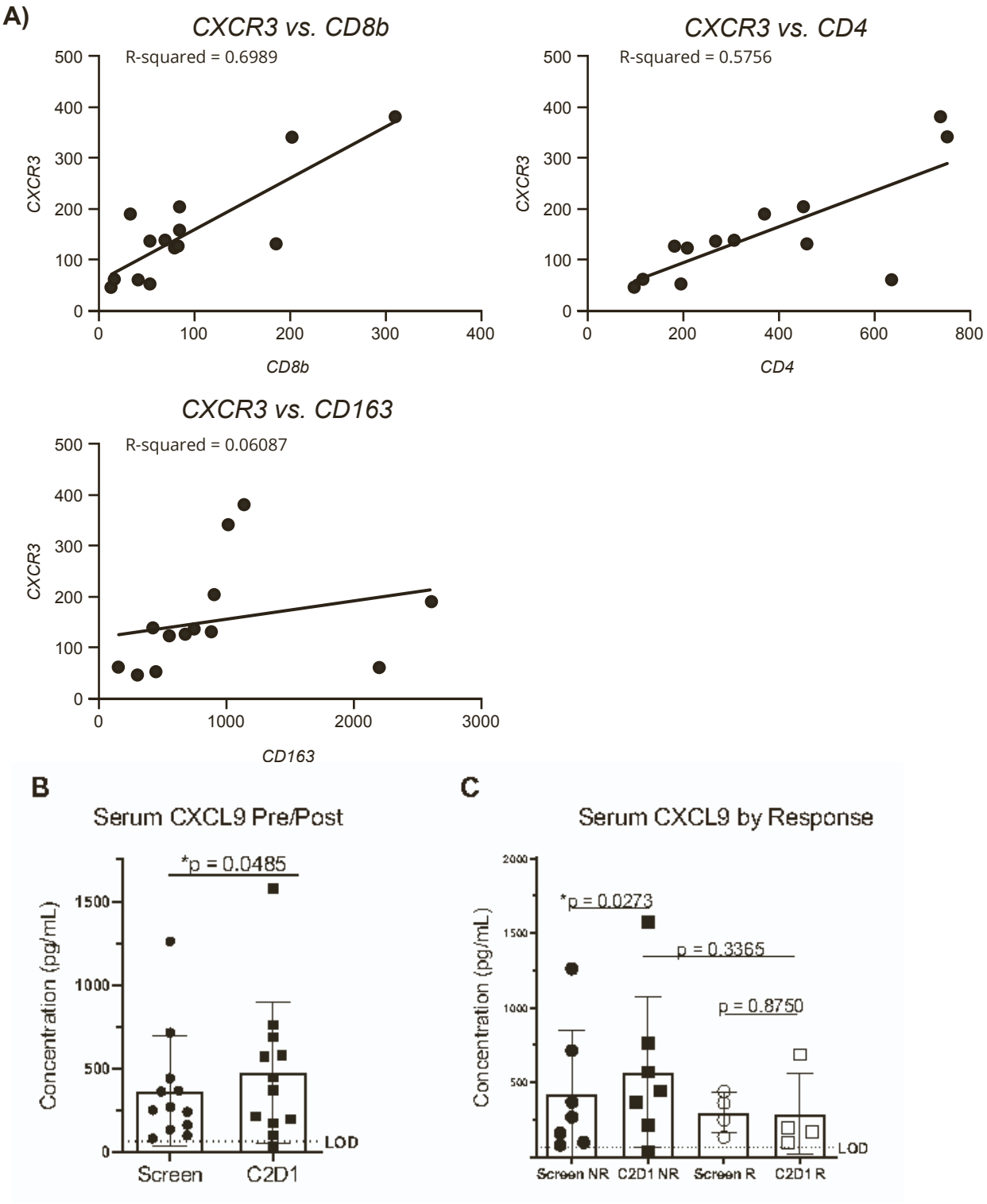

Figure S1. A) CXCR3 gene expression strongly correlates with lymphocytes. CXCR3 expression versus CD8 and CD4 expression (R^2 = 0.7 and 0.6 respectively) and CD163 expression (R^2 = 0.06) within tumors post-treatment. Gene expression was assessed by NanoString nCounter® technology (NanoString Human Immunology v2 Panel.) B) Changes in systemic levels of CXCL9 between pre- and post-treatment across all patients (n=12 pre/post matched serum samples; paired T test *p = 0.0485). C) Systemic CXCL9 levels broken out by RECISTv1.1 response (Non-responders 'NR': n=7 paired samples, paired T test *p=0.0273; responders 'R': n=4, paired T test p=0.8750).

Supplementary Figure 2

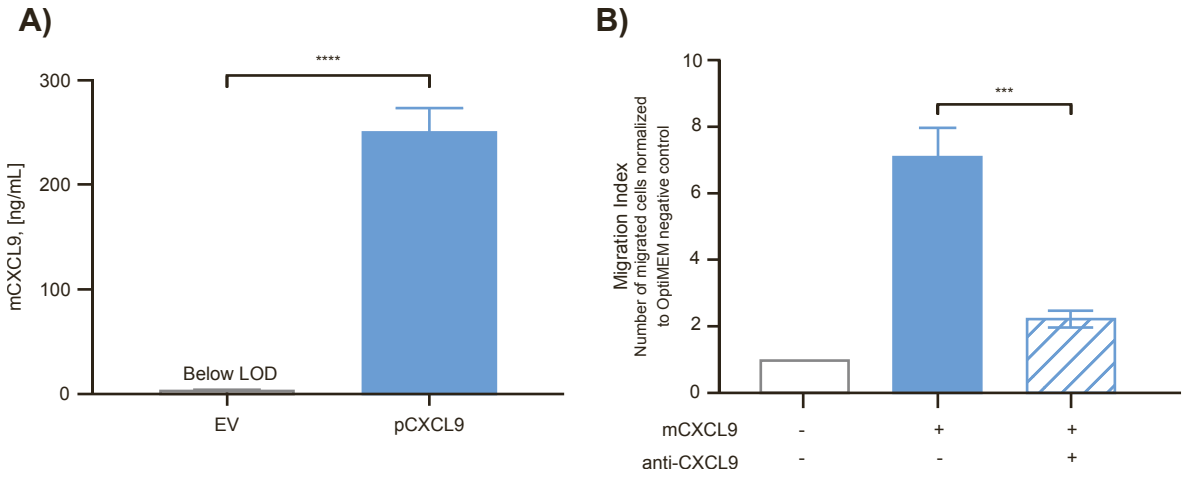

Figure S2. Murine CXCL9 plasmid expresses immunologically relevant levels of functional CXCL9 in vitro. A) Amount of mCXCL9 secreted by HEK293 cells following transient transfection with empty vector (EV) or pCXCL9 (96hr harvest; n=3; **** $p<0.0001$; Welch's T test). B) Transfection-derived mouse CXCL9 induced chemotaxis of SIINFEKL-pulsed OT-I splenocytes. Abrogation of chemotaxis was observed with the addition of anti-mCXCL9 neutralizing monoclonal antibody. (n=4; *** $p<0.0005$; Welch's T test). Migration index is defined as the number of observed chemotactic cells normalized to the number of cells that passively migrated through the membrane in the OptiMEM negative control.

Supplementary Figure 3

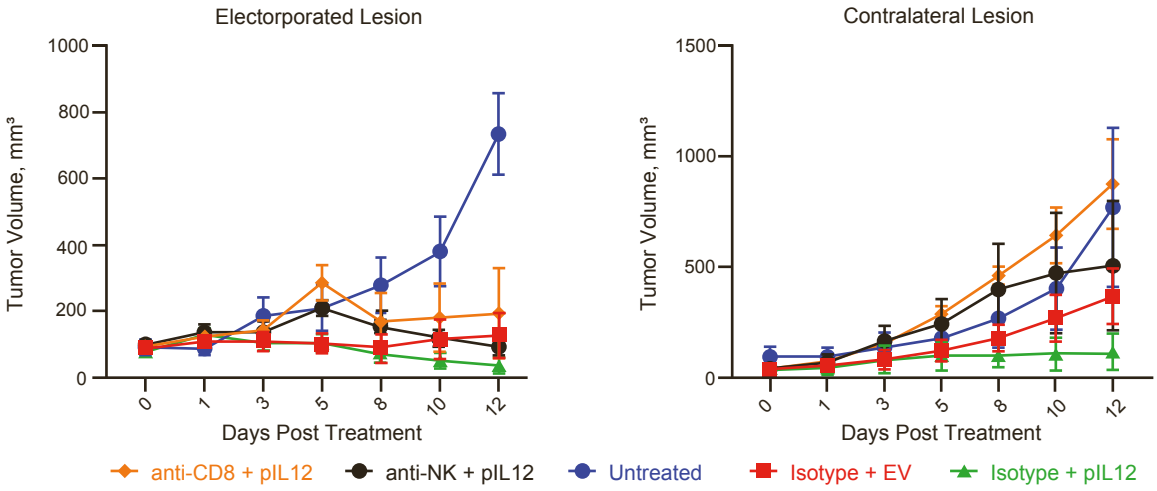

Figure S3. CD8 depletion abrogates volume control of distant tumors after intratumoral electroporation of plasmid IL-12. Tumor measurements of primary electroporated (left panel) and untreated secondary (right panel) tumors of CT26 contralateral tumor mouse models intratumorally electroporated with EV or pIL12 with or without concomitant administration of lymphocyte neutralizing antibodies.

Supplementary Figure 4

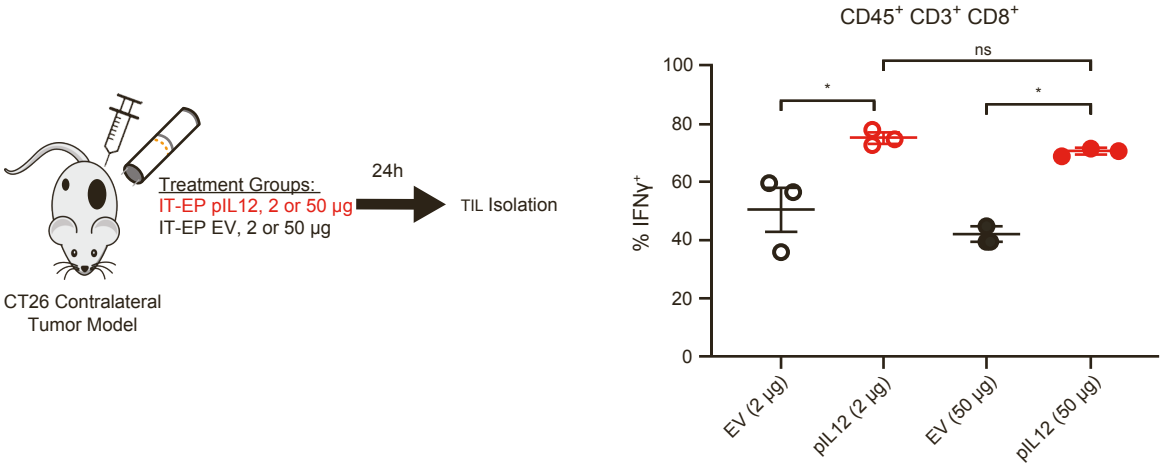

Figure S4. Intratumoral IFN- + T cells similar regardless of plasmid input amount. CT26 contralateral tumor mouse models intratumorally electroporated with 2 or 50 g of pIL12 or EV. Tumor resident CD8 + T cells were isolated and stained for intracellular IFN- .

Supplementary Figure 5

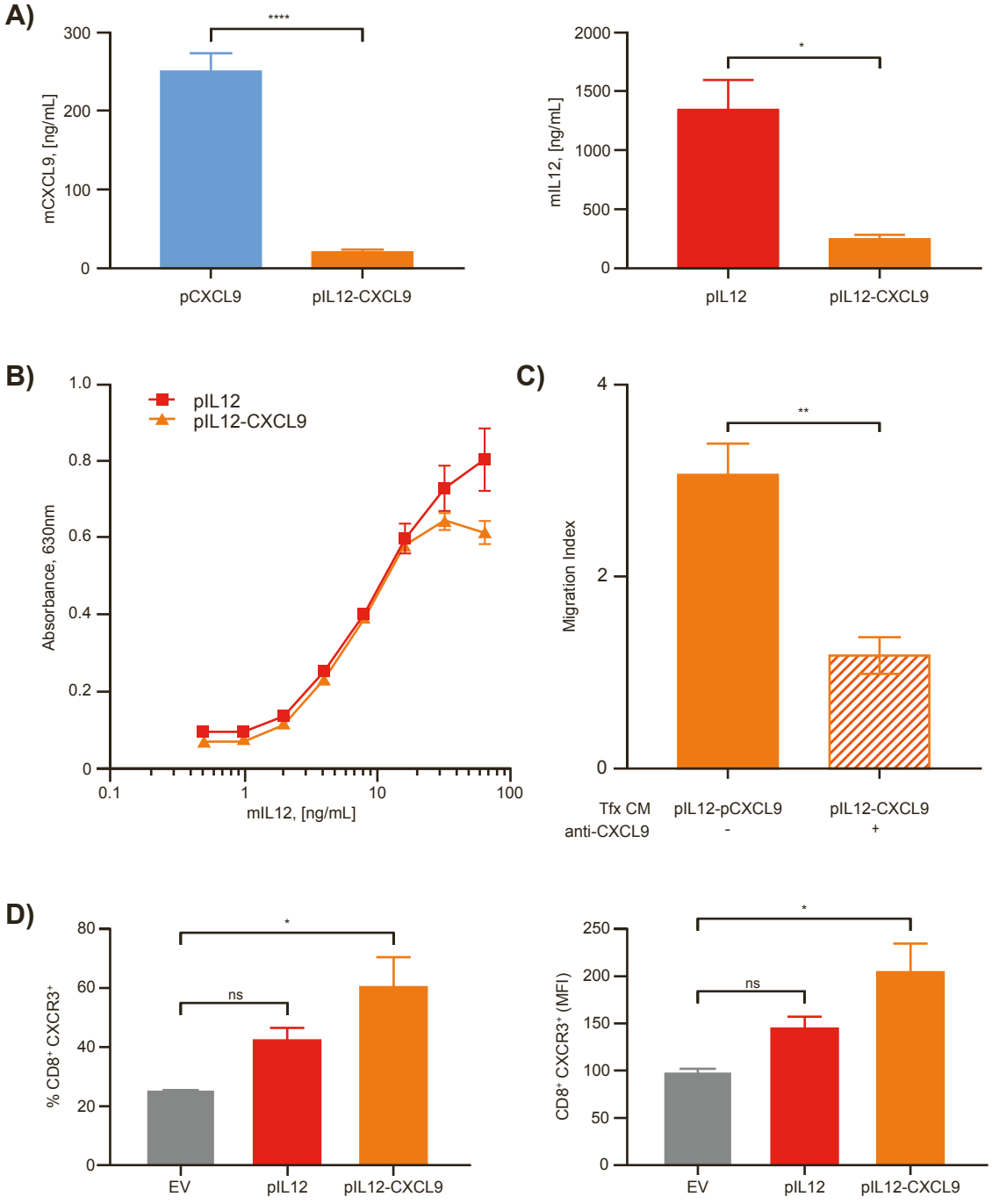

Figure S5. Expression and potency of CXCL9 and IL-12 expressed from multigene plasmid. A) Amount of mCXCL9 (left panel) and mIL12 (right panel) secreted by HEK293 cells following transient transfection with single-gene or multigene plasmids (96hr harvest; n=3; **** p<0.0001, * p<0.05; Welch's T test). B) Potencies of mIL12 from both single-gene and multigene plasmids were confirmed using a HEK-Blue reporter cell line reactive to mIL12 incubation. (**p<0.01; Welch's T test). C) Functionality of mCXCL9 from both single-gene and multigene plasmids were confirmed by their chemotactic potential. D) Percentage and MFI of CXCR3 expression on CD8+ T cells from tumors treated with EV, pIL12, or pIL12-CXCL9.

Supplementary Figure 6

A)

CT26 tumors

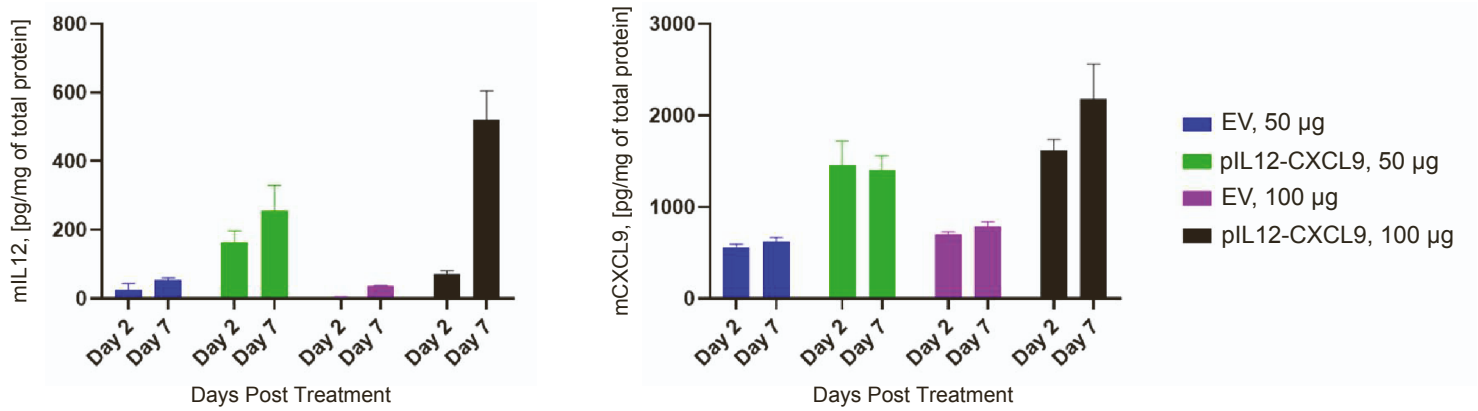

B)

B16-F10 tumors

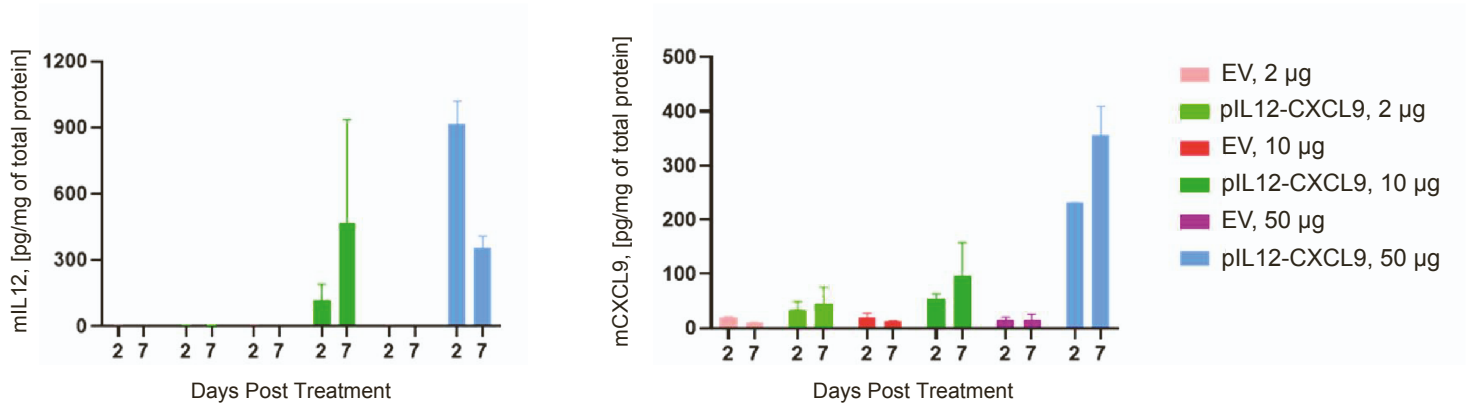

Figure S6. Intratumoral expression of IL-12 and CXCL9 protein following electroporation of pIL12-CXCL9. A) Dose response of 50 g and 100 g of EV versus the bicistronic plasmid encoding mIL12-mCXCL9. Tissue ELISAs for mIL12p70 and mCXCL9 were performed on CT26 tumor extracts 2- and 7-days post-EP. B) Dose response of 2 g, 10 g and 50 g of EV versus the bicistronic plasmid encoding IL12-CXCL9. Tissue ELISAs for mIL12p70 and mCXCL9 were performed on B16-F10 tumor extracts 2- and 7-days post-EP.